

***Ab initio* calculations of the dispersion contribution to the physisorption potential: Application to the N₂-BN system**

I. Baraille,* M. Rérat, and P. Mora

Laboratoire de Chimie Théorique et de Physico-Chimie Moléculaire, UMR CNRS 5624, FR 2606, Faculté des Sciences, Boîte Postale 1155, 64013 Pau cedex, France

(Received 22 July 2005; revised manuscript received 4 November 2005; published 6 February 2006)

We have developed an *ab initio* method to calculate the long-range dispersion coefficient for a molecule adsorbing on a surface modeled by a biperiodic slab. The variations of the dynamic polarizabilities versus imaginary frequencies of each system—considered separately—permit us to evaluate a C_4 dispersion coefficient, via the Casimir-Polder formula. The polarizability of the molecule is computed by using the time-dependent gauge-invariant variational method while the electric properties of the surface are calculated by using the periodic *ab initio* linear combination of atomic orbitals density functional theory method implemented in the CRYSTAL03 code. We have applied this method to the physisorption of the nitrogen molecule—in its ground and lowest-lying triplet states—on the (001) surface of hexagonal boron nitride. The semi-infinite crystal is simulated by slabs with different numbers of atomic layers.

DOI: [10.1103/PhysRevB.73.075410](https://doi.org/10.1103/PhysRevB.73.075410)

PACS number(s): 68.43.Bc, 73.20.At

I. INTRODUCTION

Adsorption phenomena have been intensively studied for many years, mostly due to their great practical importance in many areas like environmental analysis, separation processes and technological applications. Moreover, gas sorption is of major importance to obtain a comprehensive characterization of porous materials with respect to the specific surface area, pore size distribution and porosity.

Despite the high level of research activity in this area, the microscopic surface/adsorbate interactions remain difficult to characterize. Physisorption phenomena result from two contributions: van der Waals attractions which are reduced to London interactions for nonpolar molecules and electronic repulsion. In both experimental and theoretical approaches, such effects are difficult to quantify, primarily due to the weak nature of the binding forces between the adsorbate and the material. Some empirical adsorption isotherm equations can be used to determine the heat of adsorption but experimental data are required to determine the parameters in these models; thus this method is not predictive.

Over recent years, there has been increasing interest in using computational simulation methods to study various adsorbate-adsorbent systems, especially molecular dynamics, Monte Carlo, and grand canonical Monte Carlo approaches. Density functional theory (DFT) is another statistical mechanics model used to determine the heat of adsorption; it is based on the idea that the grand free energy of an inhomogeneous fluid can be expressed as a functional of the density profile in the pore. Nevertheless, all the above methods depend to some extent on the use of empirical potential energy functions to represent the gas/surface interactions. Many models have been proposed for this purpose, such as Steele's 10-4-3 potential.^{1,2} To gauge how realistic a given potential may be, it could be of great benefit to develop an *ab initio* approach able to predict such properties. Within this framework, the most natural method is to compute the self-consistent field electronic structure of a so-called *supersys-*

tem including the adsorbing molecule and the surface usually modeled as a cluster. Only dynamically correlated *ab initio* methods provide reliable descriptions of the mid- to long-range interaction forces that play a significant role in the physisorption. On the other hand, the calculated interaction energies are small compared to the absolute errors usually associated with such methods.

The aim of this work is to propose an alternative *ab initio* approach to compute the attractive part of the interaction potential. We have developed a method to evaluate the long-range dispersion coefficient for a molecule—nitrogen—adsorbing on a biperiodic system modeling the surface—different slabs of hexagonal boron nitride. The dipole polarizabilities of each system were calculated separately using time-dependent gauge-invariant (TDGI) variational method³ for the molecule and the sum over states method for the surface,⁴ respectively. The variations of these polarizabilities versus imaginary frequencies permit us to evaluate a C_4 dispersion coefficient, via the Casimir-Polder formula.⁵ The originality of this method is to calculate the electric properties of the surface by a periodic *ab initio* linear combination of atomic orbitals (LCAO) DFT method.^{6,7}

To test the validity of this approach, we have applied this method to the physisorption of the nitrogen molecule—in its ground and low-lying triplet states—on different slabs of boron nitride. Among gas and vapors that may be adsorbed, nitrogen remains universally preeminent.⁸ It is now possible with commercial equipment and on-line data processing to use nitrogen adsorption at 77 K both for routine quality control and for investigation of new porous materials. Considering the numerous applications of physisorption on activated carbon—a microporous form of graphite—the ideal would have been to take graphite as the adsorbate, but graphite is a semimetal with a linear crossing of the π and π^* bands at the K point of the first Brillouin zone. Thus, the static polarizability component parallel to the slab is infinite. Other developments necessary to evaluate the Casimir-Polder integral in this case, will be presented in a further paper. So to test the

reliability of our method, we consider nonconducting hexagonal boron nitride (*h*-BN) which is isoelectronic to graphite and has the same layered structure (only with different stacking). In *h*-BN, the different electronegativities of boron and nitrogen lift the degeneracy of the π bands at the *K* point and lead to an experimental band gap of 5.8 eV.⁹ Moreover *h*-BN has recently regained interest due to the synthesis of BN nanotubes,^{10–12} which can be considered as cylinders formed by rolling a single sheet of *h*-BN onto itself.

This paper is organized as follows. First we develop the theory needed for an *ab initio* evaluation of a C_4 dispersion coefficient. Then results on the physisorption of N₂ on (001) hexagonal BN slabs and bulk are presented and discussed. Finally, brief conclusions are given concerning this method.

II. THEORETICAL CONSIDERATIONS

The interaction potential between two electrically neutral and nonpolar systems *A* and *B* can be written as a multipole expansion in inverse power series of separation distance *R*. The first term in the expansion represents the instantaneous dipole-dipole interaction which is generally dominant. So the higher terms (which contribute less than 10% to the total dispersion energy) are often omitted when calculating dispersion energies.

At large distance *R* between the two systems located on the *z* axis, we only consider the first term in the development of the interaction Hamiltonian:

$$\hat{H}' = \frac{\hat{\mu}_A^x \hat{\mu}_B^x + \hat{\mu}_A^y \hat{\mu}_B^y - 2\hat{\mu}_A^z \hat{\mu}_B^z}{R^3} \quad (1)$$

where $\hat{\mu}_A^\alpha$ and $\hat{\mu}_B^\beta$ are the α and β components of the electric dipole moment operator for the interacting systems *A* and *B*, respectively. Note that the van der Waals coefficient approach is valid only if the interaction distances *R* satisfy the Le Roy criteria,¹³ i.e., for distances at which exchange potential can be neglected.

Our interest here is in studying the dispersion energy when system *B* is a biperiodic system modeling the crystal surface. In the following, B_0 denotes the reference zero cell and B_j is the general surface cell identified by the direct lattice vector \mathbf{R}_j . As shown in Fig. 1, \mathbf{R}_j can also be written as \mathbf{OO}_j , *O* and O_j being the centers of mass of the B_0 and B_j unit cells, respectively. If one regards the periodic system in its entirety as a system *B*, the dipole moment operator $\hat{\mu}_B$ can be written as the sum of dipole moments per unit cell:

$$\begin{aligned} \hat{\mu}_B &= \sum_{l \in B} q_l \hat{\mathbf{r}}_l = \sum_{\mathbf{R}_j} \sum_{l \in B_j} q_l (\hat{\mathbf{r}}_l + \mathbf{R}_j) \\ &= \sum_{\mathbf{R}_j} \hat{\mu}_B(\mathbf{R}_j) \quad \text{with} \quad \hat{\mu}_B(\mathbf{R}_j) = \sum_{l \in B_j} \mathbf{q}_l \cdot \hat{\mathbf{r}}_l \end{aligned} \quad (2)$$

since $\sum_j \mathbf{R}_j = \mathbf{0}$. \mathbf{q}_l and $\hat{\mathbf{r}}_l$ are the charge and the position vec-

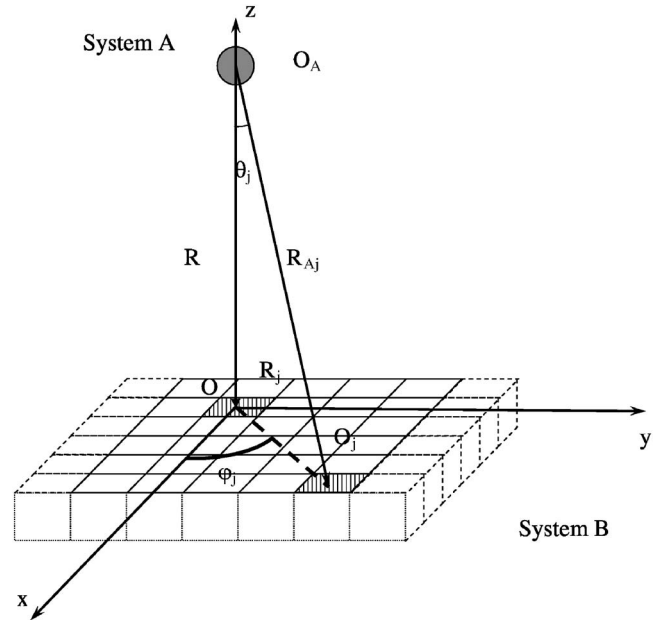


FIG. 1. Geometry of the molecule–crystalline surface system. The molecule (system *A*) is represented by a sphere. *O* and O_j are the centers of mass of the reference and current unit cells, respectively ($\mathbf{OO}_j = \mathbf{R}_j$, $\mathbf{O}_A \mathbf{O}_j = \mathbf{R}_{Aj}$, $\mathbf{O}_A \mathbf{O} = \mathbf{R}$).

tor from the point *O* in the reference frame (*O*, \mathbf{i} , \mathbf{j} , \mathbf{k}) of any particle *l* in the system *B* (nucleus or electron). The position of the *l*th particle in the unit cell B_j is given by the vector $\hat{\mathbf{r}}_l$ from point O_j .

Consequently, the interaction Hamiltonian \hat{H}' of a molecule *A* and the surface *B* of a solid, modeled as a biperiodic system is the sum of the interactions molecule *A*–unit cells B_j :

$$\hat{H}' = \sum_{\mathbf{R}_j} \hat{H}'(\mathbf{R}_j). \quad (3)$$

At this point, a so called *A*- B_j frame denoted as ($\mathbf{I}_j, \mathbf{J}_j, \mathbf{K}_j$) is defined to take the Z_j direction in the direction $\mathbf{R}_{Aj} = \mathbf{O}_A \mathbf{O}_{B_j}$, O_A being the center of mass of molecule *A* (cf. Fig. 1). Using this frame, the *A*- B_j interaction Hamiltonian can be written as

$$\hat{H}'(\mathbf{R}_j) = \frac{\hat{\mu}_A^{X_j} \hat{\mu}_B^{X_j}(\mathbf{R}_j) + \hat{\mu}_A^{Y_j} \hat{\mu}_B^{Y_j}(\mathbf{R}_j) - 2\hat{\mu}_A^{Z_j} \hat{\mu}_B^{Z_j}(\mathbf{R}_j)}{R_{Aj}^3}, \quad (4)$$

where $\hat{\mu}_A^{\alpha_j}$ and $\hat{\mu}_B^{\beta_j}(\mathbf{R}_j)$ (α or $\beta = X, Y$, or Z) are the components of the *A* and B_j dipole operators in the *A*- B_j frame, respectively.

In the case of nonpolar systems, the first-order perturbation energy is zero and the dispersion energy can be computed as the second-order perturbation energy

$$E_{A-B} = \sum_{n,m \neq 0} \frac{\langle \Psi_A^0 \Psi_B^0 | \sum_{\mathbf{R}_j} \hat{H}'(\mathbf{R}_j) | \Psi_A^n \Psi_B^m \rangle \langle \Psi_A^n \Psi_B^m | \sum_{\mathbf{R}_h} \hat{H}'(\mathbf{R}_h) | \Psi_A^0 \Psi_B^0 \rangle}{(E_A^n - E_A^0) + (E_B^m - E_B^0)} \quad (5)$$

where the unperturbed wave functions $\Psi_A^n \Psi_B^m$ are just the antisymmetrized product of the states of each isolated systems and the ground state is denoted $\Psi_A^0 \Psi_B^0$. By introducing the components of the dipole moments $\hat{\mu}_A^\alpha$ and $\hat{\mu}_B^{\alpha'}(\mathbf{R}_j)$ ($\alpha = x, y, \text{ or } z$) in the reference frame $(\mathbf{i}, \mathbf{j}, \mathbf{k})$, the interaction energy can be expressed as

$$E_{A-B} = \sum_{n,m \neq 0} \frac{1}{(E_A^n - E_A^0) + (E_B^m - E_B^0)} \left(\sum_{\mathbf{R}_j, \mathbf{R}_h} \frac{1}{R_{Aj}^3 R_{Ah}^3} \right. \\ \times \sum_{\alpha, \beta} \sum_{\alpha', \beta'} f_{jh}^{\alpha\beta\alpha'\beta'}(\theta_j, \varphi_j, \theta_h, \varphi_h) \\ \left. \times \mu_{An}^\alpha \mu_{An}^\beta \mu_{Bm}^{\alpha'}(\mathbf{R}_j) \mu_{Bm}^{\beta'}(\mathbf{R}_h) \right) \quad (6)$$

with $\mu_{An}^\alpha = \langle \Psi_A^0 | \hat{\mu}_A^\alpha | \Psi_A^n \rangle$ and $\mu_{Bm}^{\alpha'}(\mathbf{R}_j) = \langle \Psi_B^0 | \hat{\mu}_B^{\alpha'}(\mathbf{R}_j) | \Psi_B^m \rangle$.

The $f_{jh}^{\alpha\beta\alpha'\beta'}(\theta_j, \varphi_j, \theta_h, \varphi_h)$ functions are products of second-order spherical harmonic functions of the four angles

(defined in Fig. 1) $\theta_j, \varphi_j, \theta_h,$ and φ_h . They have been tabulated in Ref. 14.

At this point of the approach, it is necessary to express the wave functions of the slab as Slater determinants consisting of the crystalline orbitals $\Psi_\tau(\mathbf{k}_m)$. According to the results of Ayma *et al.*,⁴ in a periodic monodeterminantal approach, the nonzero dipole moment integrals $\mu_{Bm}^{\alpha'}(\mathbf{R}_j)$ are mono-electronic integrals such as $\langle \Psi_\tau(\mathbf{k}_m) | \hat{\mathbf{r}}^{\alpha'} | \Psi_t(\mathbf{k}_m) \rangle$ where τ and t denote occupied and unoccupied crystalline orbitals, respectively, the operator $\hat{\mathbf{r}}^{\alpha'} (=x, y, z)$ being the current position of the electron in the slab. Moreover, the corresponding transition energies are supposed to be equal to the difference $[\lambda_t(\mathbf{k}_m) - \lambda_\tau(\mathbf{k}_m)]$ between the eigenvalues of $\Psi_\tau(\mathbf{k}_m)$ and $\Psi_t(\mathbf{k}_m)$. As a consequence, the expression of the interaction energy E_{A-B} can be written as the sum

$$E_{A-B}^{\alpha\beta\alpha'\beta'} = C_6^{\alpha\beta\alpha'\beta'} \sum_{\mathbf{R}_j, \mathbf{R}_h} \frac{f_{jh}^{\alpha\beta\alpha'\beta'}(\theta_j, \varphi_j, \theta_h, \varphi_h)}{R_{Aj}^3 R_{Ah}^3}, \quad (7)$$

where

$$C_6^{\alpha\beta\alpha'\beta'} = \sum_{n \neq 0} \sum_{\mathbf{k}_m} \sum_{\tau, t} \frac{[\langle \Psi_A^0 | \hat{\mu}_A^\alpha | \Psi_A^n \rangle \langle \Psi_A^n | \hat{\mu}_A^\beta | \Psi_A^0 \rangle][\langle \Psi_\tau(\mathbf{k}_m) | \hat{\mathbf{r}}^{\alpha'} | \Psi_t(\mathbf{k}_m) \rangle \langle \Psi_t(\mathbf{k}_m) | \hat{\mathbf{r}}^{\beta'} | \Psi_\tau(\mathbf{k}_m) \rangle]}{(E_A^n - E_A^0) + [\lambda_t(\mathbf{k}_m) - \lambda_\tau(\mathbf{k}_m)]}. \quad (8)$$

$C_6^{\alpha\beta\alpha'\beta'}$ can be considered as the first van der Waals coefficient modeling the long-range interaction between the non-polar molecule A and any unit cell B_j of the slab.

The sum in expression (7) can be considered as a geometrical factor. The nondiagonal terms ($j \neq h$) cancel out. Then, the sum over diagonal terms is evaluated by calculating the infinite sums over the lattice vectors \mathbf{R}_j as integrals over the whole slab. The element of integration is

$$dS_j = \sigma R_j dR_j d\varphi_j = \sigma R^2 \frac{\sin \theta_j}{\cos^3 \theta_j} d\theta_j d\varphi_j, \quad (9)$$

where σ is the number of atoms per surface unit and R is the distance $O_A O_B$ (see Fig. 1). The resultant molecule-surface attraction potential is given by $E_{A-B} = -C_4/R^4$.

The van der Waals coefficient C_4 is computed as

$$C_4 = \frac{3\pi}{32} \sigma [3C_6^{xxxx} + 3C_6^{yyyy} + C_6^{xyxy} + C_6^{yyxx} + 4C_6^{xyyx} + 4C_6^{xxyx} \\ + 4C_6^{yyzz} + 4C_6^{zzxx} + 4C_6^{zzyy} + 8C_6^{zzzz}]. \quad (10)$$

Its determination amounts to calculating the van der Waals coefficients $C_6^{\alpha\beta\alpha'\beta'}$ to model the long-range interaction between the nonpolar molecule and any unit cell B_j of the slab.

When both systems A and B are in their ground state or in excited states for which emission is forbidden, instead of using expression (8), the $C_6^{\alpha\beta\alpha'\beta'}$ coefficients can be evaluated by performing the analytic integration involved in the Casimir-Polder formula⁵

$$C_6^{\alpha\beta\alpha'\beta'} = \frac{3}{\pi} \int_0^\infty \alpha_A^{\alpha\beta}(i\omega) \alpha_B^{\alpha'\beta'}(i\omega) d\omega, \quad (11)$$

where $\alpha_A^{\alpha\beta}(i\omega)$ and $\alpha_B^{\alpha'\beta'}(i\omega)$ are the terms of the dipole polarizability tensors of each system at imaginary frequencies ($i\omega$) in the chosen framework (see Fig. 1). This expression allows us to determine each polarizability tensor separately: $\alpha_A(i\omega)$ for the molecule and $\alpha_B(i\omega)$ for the unit cell of the biperiodic system. The great advantage of this method is to model each isolated system using different methods.

Thus the procedure that we propose to calculate the C_4 van der Waals coefficient includes three steps.

1. The polarizability tensor $\alpha_A(i\omega)$ of the molecular system A , is obtained through the time-dependent gauge-invariant method³ which is a variation-perturbation procedure including a ‘‘gauge factor’’ and taking into account the electronic correlation.

2. For the slab, we used the uncoupled method developed in our laboratory^{15,16} to compute $\alpha_B(i\omega)$. In this approach, the commonly used sum-over-states (SOS) method has been implemented, starting from the crystalline orbitals and the related eigenvalues obtained via a periodic monodeterminantal calculation. The infinite sum over all states is then replaced by a sum over occupied τ and virtual t crystalline orbitals and over \mathbf{k}_m vectors on the first Brillouin zone with a geometrical weight $\Omega(\mathbf{k}_m)$,

$$\alpha_B^{\alpha\beta}(i\omega) = 2 \sum_{\mathbf{k}_m} \Omega(\mathbf{k}_m) \sum_{\iota, \tau} \frac{\langle \Psi_{\iota}(\mathbf{k}_m) | r^{\alpha} | \Psi_{\tau}(\mathbf{k}_m) \rangle \langle \Psi_{\tau}(\mathbf{k}_m) | r^{\beta} | \Psi_{\iota}(\mathbf{k}_m) \rangle [\lambda_{\tau}(\mathbf{k}_m) - \lambda_{\iota}(\mathbf{k}_m)]}{[\lambda_{\tau}(\mathbf{k}_m) - \lambda_{\iota}(\mathbf{k}_m)]^2 + \omega^2}. \quad (12)$$

3. Finally, the $C_6^{\alpha\beta\alpha'\beta'}$ coefficients are computed by using the method proposed by Rérat and Bussery-Honvault¹⁷ to compute the van der Waals coefficient C_6 between two atoms or molecules in either their ground or excited states. The continuous functions $\alpha_A^{\alpha\beta}(i\omega)\alpha_B^{\alpha'\beta'}(i\omega)$ are fitted by using a limited number of pseudo-transition-moments and pseudoenergies for both A and B systems. Then the fitted transition moments and energies are introduced in Eq. (8) to calculate the $C_6^{\alpha\beta\alpha'\beta'}$ dispersion coefficient. This method allows one to avoid the tedious numerical integration (step and higher limit of integration) over ω and a large number of calculations of $\alpha_A^{\alpha\beta}(i\omega)$ and $\alpha_B^{\alpha'\beta'}(i\omega)$. However, use of the Casimir-Polder formula, when available, is useful to confirm the results obtained by the fit. At the end, the $C_6^{\alpha\beta\alpha'\beta'}$ coefficients are introduced in expression (10) to calculate the C_4 dispersion coefficient.

III. RESULTS AND DISCUSSION

A. Dynamic polarizability of the nitrogen molecule in the

$\tilde{X}(^1\Sigma_g^+)$ and $\tilde{A}(^3\Sigma_u^+)$ states

In the first step, we have implemented the TDGI method and computed the dynamic polarizability of nitrogen at imaginary frequencies ($i\omega$), for both the ground state $\tilde{X}(^1\Sigma_g^+)$ and the low-lying triplet state $\tilde{A}(^3\Sigma_u^+)$. In what follows, the molecular axis is the z axis.

The initial state Ψ_A^0 of the nitrogen molecule—either the ground state $\tilde{X}(^1\Sigma_g^+)$ or the first triplet state $\tilde{A}(^3\Sigma_u^+)$ —has been computed using a multireference configuration interaction (MRCI) method with the CIPSI variation-perturbation algorithm.^{18–21} For both states, the calculations were carried out at the equilibrium internuclear distance of the ground state (2.0680 a.u.), using the triple- ζ basis (p-VTZ) set due to Sadlej²² which is specific for the molecular electric properties and includes $[5s, 3p, 2d]$.

To our knowledge, these functions $\alpha_A^{zz}(i\omega)$ and $\alpha_A^{xx}(i\omega)$ have not been reported for any electronic state of N_2 , except for the static components of the ground state. Thus, to check the validity of these calculations, we compared our results with the data available in the literature. For the ground state, the components of the static polarizability [$\alpha_A^{zz}(0)=14.6$ a.u., $\alpha_A^{xx}(0)=9.7$ a.u.] are in agreement with experimental data²³ [$\alpha_A^{zz}(0)=14.8\pm 0.2$ a.u., $\alpha_A^{xx}(0)=10.2\pm 0.1$ a.u.]. In a previous study,²⁴ Mérawa *et al.* calculated the static TDGI polarizability of 14 electron diatomic molecules— N_2 , BF, and CO—in their ground states. As they used a basis set including f atomic orbitals, for the nitrogen molecule, their results [$\alpha_A^{zz}(0)=14.9$ a.u., $\alpha_A^{xx}(0)=9.9$ a.u.] are closer to the experimental data. The low-lying triplet state $\tilde{A}(^3\Sigma_u^+)$ exhibits an

inversion of anisotropy for the static polarizability components [$\alpha_A^{xx}(0)=13.04$ a.u., $\alpha_A^{zz}(0)=12.81$ a.u.]. It might be interesting to investigate the effect of such inversion on the orientation of the molecule interacting with the surface. Unfortunately, the shape of the curves $\alpha_A^{zz}(i\omega)$ and $\alpha_A^{xx}(i\omega)$ (reported in Fig. 2, for both electronic states studied) shows that the anisotropy of the ground state is restored from $\omega = 0.02$ a.u. Note that the dynamic polarizability components estimated for the ground state are higher than for the triplet state. As a consequence, the van der Waals coefficients relative to the physisorption of N_2 should be the highest for the ground state.

To our knowledge, the only experimental data available to check the validity of our calculations on the low-lying triplet state are the two electronic vertical transitions $\tilde{X}(^1\Sigma_g^+) \rightarrow \tilde{A}(^3\Sigma_u^+)$ and $\tilde{X}(^1\Sigma_g^+) \rightarrow \tilde{B}(^3\Pi)$. Our MRCI results (7.76 and 8.11 eV for $\tilde{X} \rightarrow \tilde{A}$ and $\tilde{X} \rightarrow \tilde{B}$, respectively) are in good agreement with the values reported by Nielsen *et al.*²⁵ (7.8 and 8.1 eV). Since the validity of the MRCI wave function has been confirmed, the TDGI method is expected to give accurate results for the ground and excited states of diatomic systems.²⁶ It is reasonable to think that the values of the dynamic polarizability are in the right range for this excited state.

B. The dynamic polarizability of the (001) surface of hexagonal boron nitride

In the present approximation, the adsorption of molecules on a surface is often regarded as adsorption on a single plane S_1 . To check the validity of such an approximation, we study the influence of the thickness of the slab on the dynamic polarizability at imaginary frequency.

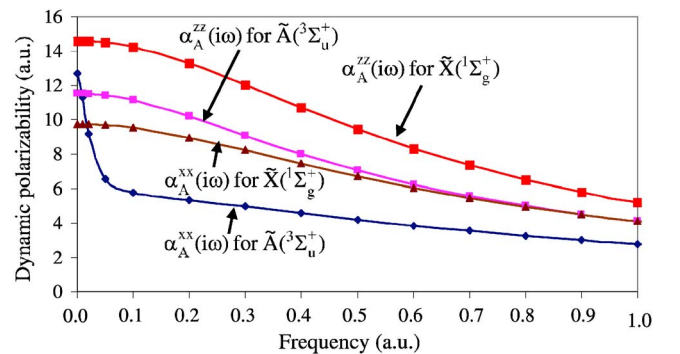


FIG. 2. (Color online) Dynamic polarizability components $\alpha_A^{zz}(i\omega)$ and $\alpha_A^{xx}(i\omega)$ at imaginary frequency for two electronic states of the nitrogen molecule, the ground state $\tilde{X}(^1\Sigma_g^+)$ and lowest-lying triplet state $\tilde{A}(^3\Sigma_u^+)$. The molecular axis is the z axis.

1. Computational details

The surface properties investigated in the present work are obtained by simulating the semi-infinite crystal by a slab model. The influence of the thickness of the slab is evaluated by considering eight systems (S_N) with different numbers of atomic layers ($N=1-5, 7, 9, 13$) parallel to the (001) face of the bulk. The resulting electric properties are compared to those of the bulk. All the nine studied systems correspond to unrelaxed slabs in which the experimental parameters of the bulk²⁷ have been maintained ($a=2.504$ Å and $c=6.661$ Å). All the periodic calculations were performed using CRYSTAL03, an *ab initio* code for periodic systems, developed by Dovesi and co-workers.^{6,7} The crystalline orbitals are expanded in terms of localized atomic Gaussian basis set, in a way similar to the LCAO method currently adopted for molecules. The eigenvalues equations are solved at the BLYP and nonlocal GGA generalized gradient approximation (GGA) levels. The GGA approach has been developed on the Perdew-Wang functionals.²⁸⁻³⁰ The BLYP functional uses Becke's exchange³¹ and the Lee-Yang-Parr correlation functionals.³² The number of k points in the first irreducible Brillouin zone in which the Hamiltonian matrix is diagonalized is 61 and 193 for the slabs and the bulk, respectively. All electron atomic basis sets are adopted to describe the atoms within the cell. The boron and nitrogen basis sets are of 6-21G* (Ref. 33) and 7-31G* (Ref. 34) type, respectively. The exponents of the most diffuse sp and d shells have been optimized considering the bulk experimental geometrical structure [$\xi(sp)=0.150$ a.u. and $\xi(d)=0.555$ a.u. for the boron atom and $\xi(sp)=0.406$ a.u. and $\xi(d)=0.764$ a.u. for the nitrogen atom].

2. Static polarizability and dielectric constant of the h-BN bulk

The first step in these calculations is to determine the conditions that lead to static values as close as possible to experimental results. Indeed, the uncoupled SOS method is well known to be not very accurate for the static polarizabilities. However, it gives the right shape for the dynamic polarizability at imaginary frequency. Static polarizability values per unit cell of the bulk have been computed at the GGA and BLYP levels. These two methods give very similar results that are given in Table I and compared to experimental values. To our knowledge, the only experimental data available in the literature are the terms of the static dielectric constant tensor [$\epsilon_B^{xx}(0)$ perpendicular to the c axis and $\epsilon_B^{zz}(0)$ parallel to the c axis].^{35,36} Note that the value of the parallel component remains dubious (2.2 for Rumyantsev *et al.*³⁶ and 4.5 for Geick *et al.*³⁵). When the local field effect is neglected or when the considered phase is dilute—which is not the case for condensed matter—the dielectric constant $\epsilon_B(0)$ is related to the static polarizability by^{37,38}

$$\alpha_B^{\alpha\beta}(0) = \frac{\epsilon_B^{\alpha\beta}(0) - 1}{4\pi n}, \quad (13)$$

where n is the number of moieties per unit volume. Note that, for semiconductors like Si,³⁹ the correction to this approximation is estimated at less than 12%. The static polarizability components calculated by using relation (12) are too

TABLE I. Static polarizability components of bulk boron nitride in a.u. [$\alpha_B^{zz}(0)$ and $\alpha_B^{xx}(0)$] at the GGA and BLYP levels. The reported values are relative to the unit cell (two BN moieties). The BLYP values are given in parentheses.

Component	Our results		Ref. 36 ^c	Ref. 35 ^d
	Operator			
	L^a	V^b		
$\sum_n f_n$	19.3 (19.4)	18.4 (18.4)		
$\alpha_B^{zz}(0)$	24.5 (24.5)	24.7 (24.8)	60.2	23.3
$\alpha_B^{xx}(0)$	24.9 (24.9)	63.1 (62.3)	76.7	64.1

^aPolarizability values computed using relation (11).

^bPolarizability values computed by integrating the hypervirial theorem in relation (11).

^cFrom $\epsilon_B^{xx}(0)=4.95$ and $\epsilon_B^{zz}(0)=4.10$ using Eq. (12).

^dFrom $\epsilon_B^{xx}(0)=4.3$ and $\epsilon_B^{zz}(0)=2.2$ using Eq. (12).

small [$\alpha_B^{xx}(0)=24.9$ a.u.] compared to the order of magnitude given by the experimental data [64.1 (Ref. 35) or 76.7 (Ref. 36) a.u.] via Eq. (13). To understand this large difference, which is not due to the local field effect alone, and even correct it, the numerator and denominator contributions to the polarizability calculation must be analyzed separately. The denominator in Eq. (12) is related to the direct gap. For h -BN, the energy gaps between the top of the valence band and K , H , and M valleys of the conduction band are of the same order of magnitude ($E_g=4.0-5.8$ eV).³⁶ At the GGA level, the computed vertical transitions (4.41, 4.77, and 5.01 eV at the H , K , and M points, respectively) are in agreement with the range proposed by Rumyantsev *et al.*³⁶ For the numerator contribution in Eq. (12), according to the rule of Thomas-Reiche-Kuhn, the sum over the oscillator strengths

$$f_{i\tau} = \frac{2}{3} \langle \Psi_i(\mathbf{k}_m) | \mathbf{r} | \Psi_\tau(\mathbf{k}_m) \rangle \langle \Psi_\tau(\mathbf{k}_m) | \mathbf{r} | \Psi_i(\mathbf{k}_m) \rangle [\lambda_\tau(\mathbf{k}_m) - \lambda_i(\mathbf{k}_m)]$$

must be the number of electrons per unit cell (24 for h -BN). When calculated at both GGA and BLYP levels, this sum is underestimated (19.3 for both methods). However, even if the correction factor applied on the transition moments to obtain the correct number of electrons improves the static polarizability values, they remain too small [$\alpha_B^{xx}(0)=32.4$ a.u.]. The other possibility to correct the numerator contribution is to apply the hypervirial theorem⁴⁰ and introduce the velocity operator (V) in relation (12), instead of length (L). In this case, the resulting values are in much better agreement with the experimental data of Rumyantsev *et al.*³⁶ [error less than 6% and 2% for $\alpha_B^{zz}(0)$ and $\alpha_B^{xx}(0)$, respectively], even if the sum on oscillator strengths is 18.4 instead of 24. Indeed, the error bars on the numerators (transition moments) and denominators (crystalline energies) are

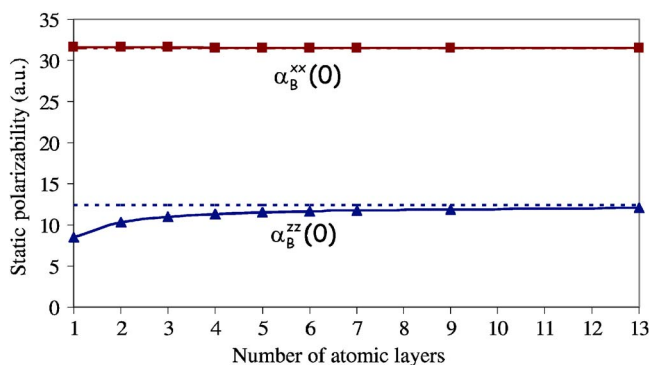


FIG. 3. (Color online) Static polarizability components $\alpha_B^{zz}(0)$ and $\alpha_B^{xx}(0)$ of hexagonal boron nitride plotted as a function of the number of atomic layers in the slab. The surface plane is the xOy plane. The dotted line represents the static polarizability $\alpha_B^{zz}(0)$ term for the bulk (12.4 a.u. or bohr³).

compensated by introducing the velocity operator. In the following, we thus adopted these conditions to calculate the dynamic polarizabilities of the S_N slabs. Note that, whatever the assumptions of the calculations, our results on the $\alpha_B^{zz}(0)$ component are 50% smaller than the data of Geick *et al.*³⁵ This could be due to the basis set used in this work which is not sufficiently extended in the z direction.

3. Static and dynamic polarizabilities of the S_N slabs

The values of the static polarizability components calculated for the S_N slabs are almost the same in both BLYP and GGA methods. In the following, we only discuss the GGA results. In Fig. 3, we report the variation of each static polarizability component per BN moiety versus the number of layers N in the slabs. Due to the layered structure of h -BN, for any slab, the value of the parallel component [$\alpha_B^{xx}(0)$] is the same as for the bulk (31.6 a.u.). The static perpendicular component [$\alpha_B^{zz}(0)$] increases from 8.5 a.u. for S_1 to 12.0 a.u. for S_{13} . Convergence within 5% of the bulk value (12.4 a.u.) is reached at $N=7$ (11.8 a.u.). Note that the value obtained for S_1 (8.5 a.u.) is relatively low compared to the bulk (12.4 a.u.). The basis set may be not extended enough to correctly translate the deformation of the electronic cloud perpendicular to the slab. In this case, the model of adsorption of molecules on BN should include several layers.

The $\alpha_B^{xx}(i\omega)$ and $\alpha_B^{zz}(i\omega)$ components per BN moiety computed at the GGA level are reported in Figs. 4 and 5 respectively, for the different S_N slabs ($N=1-13$) and the bulk. For the component parallel to the slab (see Fig. 4), all the curves are very close, due to the layered structure of h -BN. For the perpendicular component, all the curves present the same shape but are differentiated compared to the bulk (see Fig. 5). When the number of layers increases, the corresponding curves converge to the bulk.

C. The dispersion coefficient C_4 for the physisorption of N_2 on the h -BN (001) surface

When considering the perpendicular approach of the N_2 molecule (N-N molecular axis along the c axis) toward the

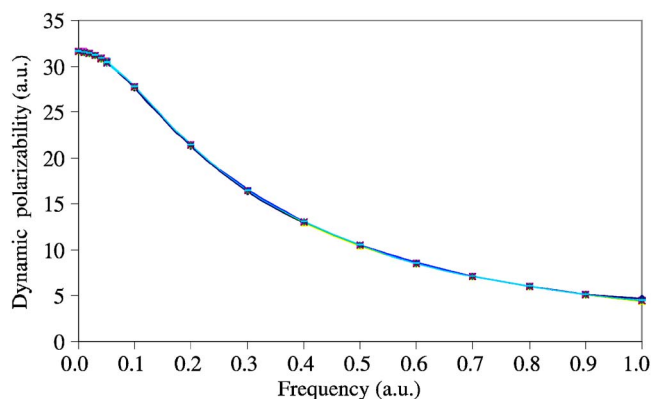


FIG. 4. (Color online) Dynamic polarizability [$\alpha_B^{xx}(i\omega)$] component at imaginary frequency, parallel to the surface plane, for the slabs and the bulk of hexagonal boron nitride.

(001) BN surface (plane xOy), the expression (10) of the van der Waals coefficient C_4 becomes

$$C_4^{\text{pe}} = \frac{3\pi}{4} \sigma (C_6^{\text{xxxx}} + C_6^{\text{xxzz}} + C_6^{\text{zzxx}} + C_6^{\text{zzzz}})$$

while, in the parallel approach with the N-N molecular axis along the Ox direction,

$$C_4^{\text{pa}} = \frac{3\pi}{8} \sigma (C_6^{\text{xxxx}} + C_6^{\text{xxzz}} + 3C_6^{\text{zzxx}} + 3C_6^{\text{zzzz}})$$

with $\sigma=0.05157$ bohr⁻².

For each N_2 electronic state [$\tilde{X}(^1\Sigma_g^+)$ and $\tilde{A}(^3\Sigma_u^+)$] and each h -BN slab, the four $C_6^{\alpha\alpha\beta\beta}$ coefficients were computed by using the fit with four pairs of transition moments and energies for A and B . As the variations of the $\alpha_B^{xx}(i\omega)$ components are the same whatever the number of layers in the slab, it is sufficient to consider only the bulk case to compute the C_6^{xxxx} and C_6^{zzxx} coefficients. As shown in Table II, the C_6^{xxxx} and C_6^{zzxx} values we found for both S_1 slab and the bulk are almost the same. On the other hand, Fig. 6 reports the variation of both coefficients C_6^{xxzz} and C_6^{zzzz} according to the number

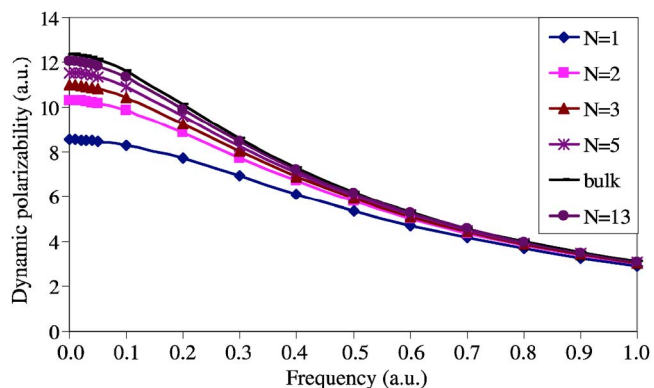


FIG. 5. (Color online) Dynamic polarizability component $\alpha_B^{zz}(i\omega)$ at imaginary frequency, perpendicular to the surface plane, for the slabs and the bulk of hexagonal boron nitride. The surface plane is the xOy plane.

TABLE II. van der Waals coefficients C_6^{xxxx} and C_6^{zzxx} (a.u.) modeling the long-range interaction between N_2 and any unit cell of the S_1 slab or bulk boron nitride. For N_2 , both the ground state $\tilde{X}(^1\Sigma_g^+)$ and low-lying triplet state $\tilde{A}(^3\Sigma_u^+)$ have been considered.

	$\tilde{X}(^1\Sigma_g^+)$		$\tilde{A}(^3\Sigma_u^+)$	
	C_6^{xxxx}	C_6^{zzxx}	C_6^{xxxx}	C_6^{zzxx}
S_1	18.7	26.7	12.4	20.6
Bulk	18.6	26.7	12.4	20.6

of layers in the slab, for both the ground state $\tilde{X}(^1\Sigma_g^+)$ and the first triplet state $\tilde{A}(^3\Sigma_u^+)$ of N_2 . The two coefficients (C_6^{xxzz} and C_6^{zzzz}) vary as

$$C_6^\infty \left(1 - \frac{A_1}{(N+1)} - \frac{A_2}{(N+1)^2} - \frac{A_3}{(N+1)^3} \right),$$

where C_6^∞ , A_1 , A_2 , and A_3 are constants set up by a least-squares fit, in each case. The C_6^∞ constants represent the asymptotic behavior of the curves and should correspond to the values of the coefficients C_6^{xxzz} and C_6^{zzzz} for an infinite number of layers, i.e., the bulk. Indeed, the fitted values are closed to those found for the h -BN bulk [$C_6^{xxzz}=9.7$ a.u. and $C_6^{zzzz}=13.6$ a.u. for the $\tilde{X}(^1\Sigma_u^+)$ electronic state and $C_6^{xxzz}=6.4$ a.u. and $C_6^{zzzz}=10.6$ a.u. for the $\tilde{A}(^3\Sigma_u^+)$ one].

The resulting dispersion coefficients C_4^{pa} (N_2 parallel to the c axis) and C_4^{pe} (N_2 perpendicular to the c axis) are reported in Table III, for both electronic states of N_2 . As expected, both C_4^{pa} and C_4^{pe} values are higher for the ground state of N_2 . Moreover, at long distance, the parallel approach of N_2 to the BN crystalline surface is favored, for both

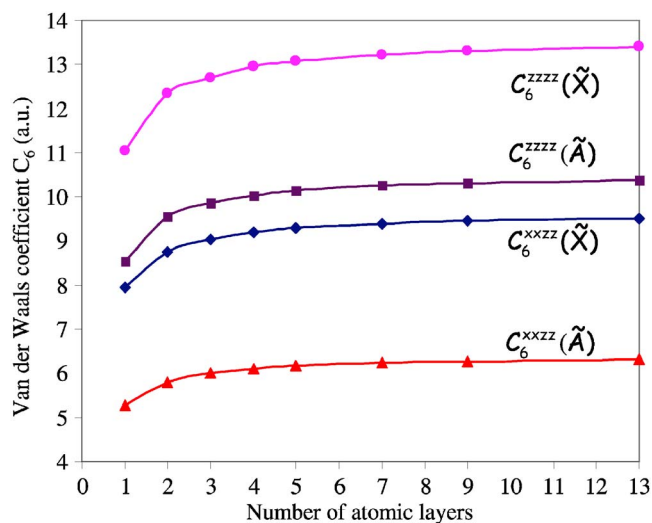


FIG. 6. (Color online) van der Waals coefficients C_6^{xxzz} or C_6^{zzzz} relative to the interaction between the nitrogen molecule and any unit cell of the h -BN crystalline surface plotted as a function of the number of the atomic layers in the slab. Both the ground state $\tilde{X}(^1\Sigma_g^+)$ and low-lying triplet state $\tilde{A}(^3\Sigma_u^+)$ of N_2 are considered.

TABLE III. C_4 dispersion coefficient (in a.u.) for N_2 , either in its ground state $\tilde{X}(^1\Sigma_g^+)$ or in its low-lying triplet state $\tilde{A}(^3\Sigma_u^+)$ adsorbing on (001) different slabs S_N of hexagonal boron nitride. (N is the number of atomic layers in the slab, the bulk corresponding to N infinite.) The exponents “pa” or “pe” mean that N_2 is parallel or perpendicular to the BN surface.

N	$\tilde{X}(^1\Sigma_g^+)$		$\tilde{A}(^3\Sigma_u^+)$	
	C_4^{pa}	C_4^{pe}	C_4^{pa}	C_4^{pe}
1	8.49	7.81	6.39	4.65
2	8.78	8.07	6.60	4.71
3	8.86	8.15	6.67	4.74
4	8.92	8.19	6.71	4.75
5	8.94	8.22	6.73	4.76
7	8.98	8.25	6.76	4.77
9	9.00	8.27	6.77	4.77
13	9.02	8.29	6.79	4.78
Bulk	9.06	8.33	6.82	4.79

$\tilde{X}(^1\Sigma_g^+)$ and $\tilde{A}(^3\Sigma_u^+)$ states. Information on the interaction parameters on BN is sparse. To our knowledge, only a few experimental studies^{41,42} were devoted to the physisorption of N_2 on boron nitride BN. The only attempt to represent the interaction potential for a single molecule N_2 (in its ground state) on the BN substrate is based on a modified Lennard-Jones form which accounts for the electronic distribution in the BN surface.⁴³ The resulting C_6 van der Waals coefficient (either 132 a.u. if using combination rules of homogeneous atomic pairs or 91.6 a.u. if correcting the Lennard-Jones parameters by an effective bulk scale factor) does not directly account for the anisotropies of the N_2 and BN polarizabilities. It corresponds to a sort of “isotropic” coefficient that could be calculated from our theoretical data as

$$\frac{2}{3}(4C_6^{xxxx} + 2C_6^{xxzz} + 2C_6^{zzxx} + C_6^{zzzz}).$$

The resulting values (103.4 and 107.4 a.u. for the monolayer slab and the bulk, respectively) are in better agreement with the model accounting for the presence of the surrounding solid.

IV. CONCLUSION

In this work, we have developed an *ab initio* method to calculate the long-range dispersion coefficient for a molecule adsorbing on a surface modeled by a biperiodical system. We have applied this method to the physisorption of N_2 on (001) surface of hexagonal boron nitride. The most important point is that the molecule and the surface are studied separately, in contrast to direct *ab initio* calculations using the supersystem approach. Thus, different computational methods may be used to investigate the electronic properties of the molecule and of the crystalline surface. This approach should give a more reliable description of the physisorption phenomena at dissociation than the supersystem method—the computed in-

teraction energy is of the same order as the error bars usually associated with total energies. Moreover, in contrast to the commonly adopted model, the boron and nitrogen atoms are not considered as individual atoms in the evaluation of the interaction potential. The C_4 parameter accounts for the effect of the crystalline field on the BN entity. This method also permits study of the physisorption of the molecule in any excited state that does not emit. The application could be an inversion of the orientation of the physisorbed molecule in the excited state, respected to the ground state.

Actually, the limitation of this approach lies in the calculation of the polarizability components per unit cell of the surface using the uncoupled sum over states method without any local field correction. Moreover, the atomic basis set used in LCAO DFT periodic calculations is not extended enough to represent the deformation of the electronic cloud. However, we adopt conditions (choice of operator, correction on oscillator strengths, gap) that lead to static values of po-

larizability as close as possible to experimental results. When these data are not available, coupled methods like the finite-field perturbation method included in the CRYSTAL03 program⁴⁴ can be used to obtain an accurate static dielectric constant. In this work, we estimate the error on our C_4 values is about 10%, corresponding to the error on the estimation of the static polarizability of the surface when using Eq. (3) (i.e., when neglecting the local field effect).

Study of the physisorption of N_2 on BN has shown that, at long range, the perpendicular approach of the N_2 molecule (in both the ground and the lowest-lying triplet states) to the surface is less favorable than the parallel orientation. So the adsorption of the excited state of N_2 does not change the orientation of the molecule, despite the inversion of anisotropy of the static polarizability relative to the ground state. Unlike graphite, information on the interaction parameters on BN is sparse and our method provides relatively accurate values.

*Corresponding author. Present address: LCTPCM, Université de Pau et des Pays de l'Adour, I.F.R. Rue Jules Ferry, BP27540, 64075 PAU, France. FAX: +33-559407862. Email address: isabelle.baraille@univ-pau.fr

¹W. A. Steele, Surf. Sci. **36**, 317 (1973).

²W. A. Steele, J. Phys. (Paris), Colloq. **38**, C4-61 (1974).

³M. Rérat, M. Mérawa, and C. Pouchan, Phys. Rev. A **45**, 6263 (1992).

⁴D. Ayma, J. P. Campillo, M. Rérat, and M. Causà, J. Comput. Chem. **18**, 1253 (1997).

⁵H. B. G. Casimir and D. Polder, Phys. Rev. **73**, 360 (1948).

⁶V. R. Saunders, R. Dovesi, C. Roetti, R. Orlando, C. M. Zicovich-Wilson, N. M. Harrison, K. Doll, B. Civalleri, I. J. Bush, P. D'Arco, and M. Llunell, Computer Code CRYSTAL 03 (Università di Torino, Torino, 1996).

⁷C. Pisani, R. Dovesi, and C. Roetti, in *Hartree-Fock Ab Initio Treatment of Crystalline Solids*, Lecture Notes in Chemistry, Vol. 48 (Springer-Verlag, Heidelberg, 1988).

⁸K. Sing, Colloids Surf., A **187-188**, 3 (2001).

⁹Y. H. Kim, K. J. Chang, and S. G. Louie, Phys. Rev. B **63**, 205408 (2001).

¹⁰A. Rubio, J. L. Corkill, and M. L. Cohen, Phys. Rev. B **49**, 5081 (1994).

¹¹X. Blase, A. Rubio, S. G. Louie, and M. L. Cohen, Europhys. Lett. **28**, 335 (1994).

¹²N. G. Chopra, R. J. Luyken, K. Cherrey, V. H. Crespi, M. L. Cohen, S. G. Louie, and A. Zettl, Science **269**, 966 (1995).

¹³R. J. Le Roy, Can. J. Phys. **52**, 246 (1974).

¹⁴M. Patxi, Ph.D. thesis, Université de Pau et des Pays de l'Adour, France, 2004.

¹⁵D. Ayma, Ph.D. thesis, Université de Pau et des Pays de l'Adour, France, 1997.

¹⁶C. Darrigan, Ph.D. thesis, Université de Pau et des Pays de l'Adour, France, 2001.

¹⁷M. Rérat and B. Bussery-Honvault, Mol. Phys. **101**, 373 (2003).

¹⁸B. Huron, J. P. Malrieu, and P. Rancurel, J. Chem. Phys. **58**, 5745 (1973).

¹⁹B. Huron and P. Rancurel, Chem. Phys. Lett. **13**, 515 (1972).

²⁰P. Rancurel, B. Huron, L. Praud, J. P. Malrieu, and G. Berthier, J. Mol. Spectrosc. **60**, 259 (1976).

²¹J. P. Malrieu and F. Spiegelmann, Theor. Chim. Acta **52**, 55 (1979).

²²A. J. Sadlej, Collect. Czech. Chem. Commun. **53**, 1995 (1988); Theor. Chim. Acta **79**, 123 (1992); Theor. Chim. Acta **81**, 45 (1992); **81**, 339 (1992).

²³A. Kumar and W. J. Meath, Theor. Chim. Acta **54**, 131 (1992).

²⁴M. Mérawa, M. Rérat, and A. Lichanot, Int. J. Quantum Chem. **71**, 63 (1999).

²⁵E. S. Nielsen, P. Jørgensen, and J. Oddershede, J. Chem. Phys. **73**, 6238 (1980).

²⁶M. Mérawa and M. Rérat, Eur. Phys. J. D **17**, 329 (2001).

²⁷E. K. Sichel, R. E. Miller, M. S. Abrahams, and C. J. Buiocchi, Phys. Rev. B **13**, 4607 (1976).

²⁸J. P. Perdew and Y. Wang, Phys. Rev. B **33**, R8800 (1986).

²⁹J. P. Perdew and Y. Wang, Phys. Rev. B **40**, 3399 (1989).

³⁰J. P. Perdew and Y. Wang, Phys. Rev. B **45**, 13244 (1992).

³¹A. D. Becke, J. Chem. Phys. **98**, 5648 (1993).

³²C. Lee, W. Yang, and R. G. Parr, Phys. Rev. B **37**, 785 (1988).

³³R. Orlando, R. Dovesi, and C. Roetti, J. Phys.: Condens. Matter **2**, 7769 (1990).

³⁴R. Pandey, J. E. Jaffe, and N. M. Harrison, J. Phys. Chem. Solids **55**, 1357 (1994).

³⁵R. Geick, C. H. Perry, and G. Rupprecht, Phys. Rev. **146**, 543 (1966).

³⁶S. L. Rumyantsev, M. E. Levinshstein, A. D. Jackson, S. N. Mohammad, G. L. Harris, M. G. Spencer, and M. S. Shur, in *Properties of Advanced Semiconductor Materials GaN, AlN, InN, BN, SiC, SiGe*, edited by M. E. Levinshstein, S. L. Rumyantsev, and M. S. Shur (John Wiley & Sons, New York, 2001), pp. 67–92.

³⁷S. L. Adler, Phys. Rev. **126**, 413 (1962).

³⁸N. Wiser, Phys. Rev. **129**, 62 (1963).

³⁹S. Baroni and R. Resta, Phys. Rev. B **33**, 7017 (1986).

⁴⁰C. Cohen-Tannoudji, B. Din, and F. Lanoë, *Mécanique Quantique*

(Herman, Paris, 1973), Vol. 2.

⁴¹M. T. Alkhafaji, P. Shrestha, and A. D. Migone, Phys. Rev. B **50**, 11088 (1994).

⁴²P. Shrestha and A. D. Migone, Phys. Rev. B **54**, 17102 (1996).

⁴³W. Li, P. Shrestha, A. D. Migone, A. Marmier, and C. Girardet, Phys. Rev. B **54**, 8833 (1996).

⁴⁴C. Darrigan, M. Rérat, G. Mallia, and R. Dovesi, J. Comput. Chem. **24**, 1305 (2003).